05,09

^{57}Fe NMR study of layered chalcogenide Fe_7S_8

© M.E. Kashnikova[1,2], N.A. Utkin[1,2], V.V. Ogloblichev[1,¶], A.F. Sadykov[1], A.G. Smolnikov[1], Yu.V. Piskunov[1], I.Yu. Arapova[1], N.V. Selezneva[2], N.V. Baranov[1,2]

[1] M.N. Mikheev Institute of Metal Physics, Ural Branch, Russian Academy of Sciences, Yekaterinburg, Russia
[2] Ural Federal University after the first President of Russia B.N. Yeltsin, Yekaterinburg, Russia

¶ E-mail: ogloblichev@imp.uran.ru

Received October 11, 2024
Revised October 24, 2024
Accepted October 25, 2024

The paper presents the results of a nuclear magnetic resonance (NMR) study of the magnetically ordered phase of layered chalcogenide Fe_7S_8 (pyrrhotite) on iron nuclei ^{57}Fe in a zero external magnetic field in the temperature range $T = 4.2-295$ K. The obtained NMR spectra on the ^{57}Fe nuclei represent several lines in the frequency range $\Delta\nu = 30-50$ MHz. The absence of iron ions in the Fe^{3+} state in Fe_7S_8 is proven. The presence of several magnetically nonequivalent positions of iron ions, differing in the number and location of vacancies near them, is detected. The rates of spin-spin and spin-lattice relaxation of the nuclear magnetic moments of ^{57}Fe are measured in different frequency regions of the spectrum at different temperatures. Local magnetic fields on iron nuclei are determined and the magnetic moment of Fe ions is estimated. It is shown that the ^{57}Fe spectra in the Fe_7S_8 chalcogenide can be interpreted in the 4*C*-type superstructure model. The results obtained in this work expand the prospects for the use of NMR spectroscopy in the mining industry, in particular in the detection, separation and real-time selection of ore fragments containing pyrrhotite Fe_7S_8.

Keywords: transition metal chalcogenides, layered defective structure, nuclear magnetic resonance, ^{57}Fe, pyrrhotite, local magnetic field, 4*C*-type structure.

DOI: 10.61011/PSS.2024.11.60091.260

1. Introduction

The compound Fe_7S_8 studied in this work belongs to the family of iron sulfide minerals with the formula $Fe_{1-x}S$, where x varies in the range from 0 to 0.125. Fe_7S_8 also has its own name — pyrrhotite along with the initial composition with $x = 0$, troilite which is an FeS mineral without vacancies in cationic layers. The largest number of papers is devoted specifically to the study of the compound Fe_7S_8 among the entire $Fe_{1-x}S$ series with the ordering of vacancies in cation layers. Monoclinic structure is a stable phase of this composition at room temperature. It is a superstructure of the 4*C*-type ordering $[(2\sqrt{3})a_0 \times 2a_0 \times 4c_0]$, which is described by the spatial group C2/*c* (a_0 and c_0 are the parameters of NiAs lattice cell) [1–4].

The crystal structure of pyrrhotite Fe_7S_8 consists of completely filled layers of sulfur located between planes of iron atoms (Figure 1). The latter have vacancies in every second layer of Fe. The Fe magnetic moments are oriented parallel to each other inside each plane, but antiparallel with respect to the magnetic moments in neighboring layers. The presence of vacancies in every second Fe layer leads to incomplete compensation of magnetic moments and ferrimagnetic order (the Curie temperature is about 590 K [1]). Recently, iron-based chalcogenides Fe_7X_8 (X = S, Se, Te) have been of particular interest to researchers, since their magnetic properties strongly depend on substitutions both in Fe sublattices [5,6] and in chalcogen sublattices [5].

For example, the replacement of iron in $Fe_{7-y}M_yX_8$ (X = S, Se) with atoms of other 3*d* metals (M = Ti, Co, V) leads to a decrease of magnetization and Curie temperature [7,8]. At the same time, this is not observed when Fe is replaced by chromium or manganese atoms.

It is quite difficult to get a detailed picture of the ordering of vacancies in the iron layers. The analysis of hyperfine magnetic interactions (HMI) in iron ions is a promising direction in solving this problem. Mossbauer spectroscopy using ^{57}Fe isotope allows obtaining information about HMI. The presence of vacancies in the iron layers leads to a different immediate environment of a particular Fe ion, which is reflected in different local magnetic fields on the nuclei of these ions. In turn, this induces the occurrence of several lines in the Mossbauer spectra, each of which will correspond to a specific local field, and hence to a specific immediate environment of Fe ions [9–11]. However, when analyzing the Mossbauer spectra, it is necessary to take into account the electric quadrupole interaction, since the excited state of ^{57}Fe has a nuclear spin $I = 3/2$. There is no such problem in the case of nuclear magnetic resonance (NMR) using a stable ^{57}Fe nucleus as an NMR probe, which has a nuclear spin $I = 1/2$ and, therefore, does not enter into an electric quadrupole interaction. The shape of the NMR line of ^{57}Fe nuclei directly reflects the distribution of local

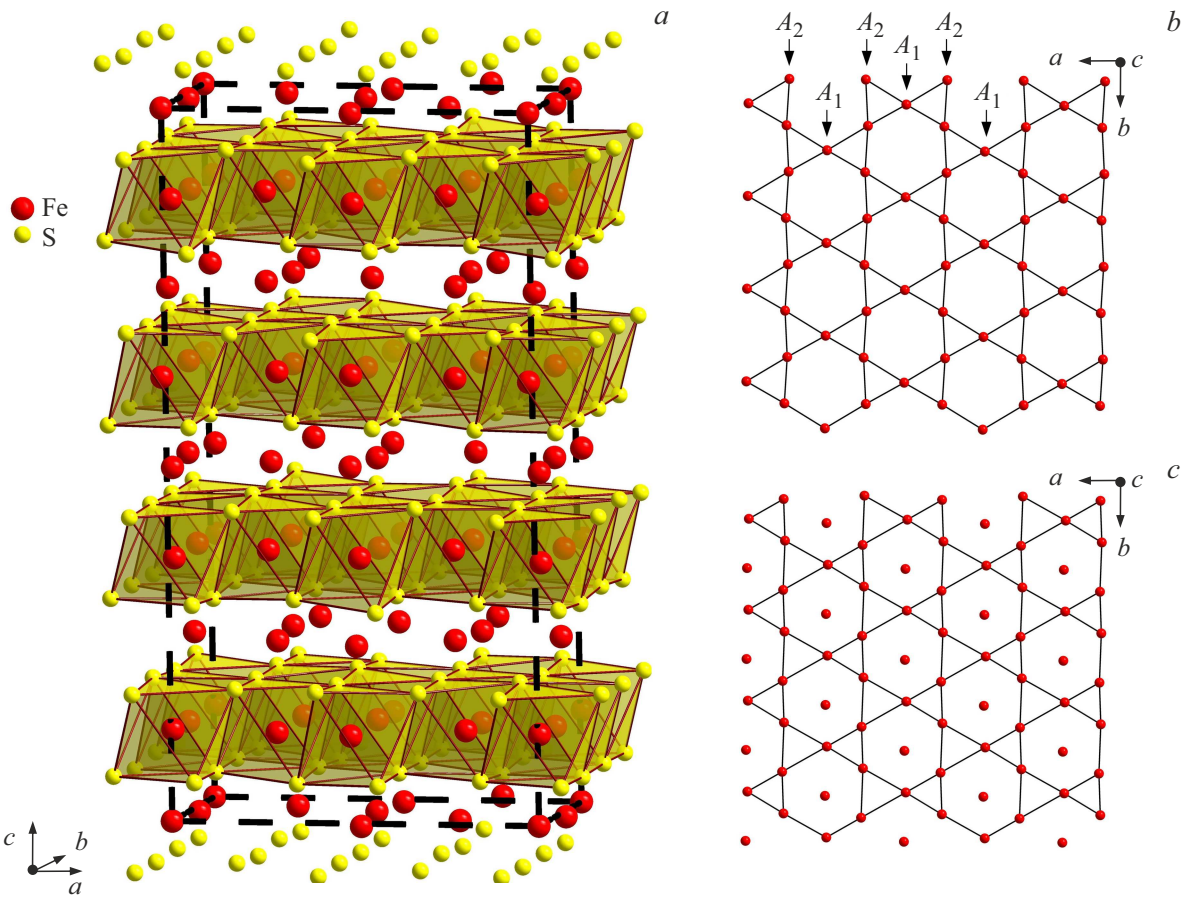

Figure 1. *a*) 4*C*-type structure and ordering of vacancies in pyrrhotite Fe_7S_8. Iron cations in the layer of ordered vacancies are shown without octahedra, and iron cations in the fully occupied layer are shown in the center of shaded octahedra FeS_6. Dotted lines indicate the trigonal lattice cell C2/*c*, illustrating the repetition of four blocks of layers of iron and sulfur in the direction perpendicular to planes *ab*. *b*) A layer of iron cations with ordered vacancies. *c*) A layer of iron cations without vacancies.

magnetic fields (H_{loc}). For example, the values of H_{loc} in tetrahedral and octahedral positions in magnetite (Fe_3O_4) differ by about 6%, and ^{57}Fe NMR lines for these two positions are very well resolved [12].

It is reported in Ref. [13] that an NMR signal was detected on ^{57}Fe nucleus in pyrrhotite Fe_7S_8 in a zero external magnetic field at room temperature. The authors observed one asymmetric peak at a frequency of $\nu_{res} = 42.03$ MHz. Unfortunately, they were unable to observe any other peaks, and the relaxation parameters were also not determined. Nevertheless, one of the conclusions of the study is the assumption that the presented NMR spectroscopy method can be appropriately adapted in the mining industry for the real-time detection and selection of ore fragments containing pyrrhotite [14,15]. For example, the nickel-rich mineral pentlandite $(Fe,Ni)_9S_8$ contains pyrrhotite. Recording of the NMR signal at a frequency of 42.03 MHz, corresponding to pyrrhotite, will indicate the presence of ore $(Fe,Ni)_9S_8$. This prospecting method can be used in the main nickel sulfide deposits. We performed measurements in a wider frequency range in this paper to search for NMR signals from ^{57}Fe nuclei, and we also studied the relaxation characteristics of the magnetic moments of iron nuclei. The data obtained are necessary both for further fundamental study of Fe_7S_8 and materials based on it, and for their practical application.

2. Samples and research methods

The polycrystalline sample Fe_7S_8 was obtained by solid-phase synthesis in evacuated quartz ampoules. The mixture of the initial elements was slowly heated to a temperature of 950 °C during a day and annealed at this temperature for 2 weeks. After that, homogenization annealing was performed at $T = 800$°C for one week, followed by slow cooling. X-ray certification of the obtained samples was conducted using Bruker D8 ADVANCE diffractometer with CuKα radiation. Diffractograms of the studied sample of pyrrhotite Fe_7S_8, as well as the results of measurements of the field and temperature dependences of the sample magnetization in the temperature range of 2–1000 K are presented in Refs. [16,17]. X-ray diffraction analysis of a polycrystalline sample of Fe_7S_8 showed that it does not contain extraneous phases, has a layered monoclinic

crystal structure with a vacancy superstructure of 4*C*-type, described by the spatial group C2/*c* with the lattice cell parameters $a = 12.000(6)$ Å, $b = 6.989(3)$ Å, $c = 22.801(0)$ Å and $\beta = 90.732°$. These values of the crystal lattice parameters are in good agreement with the previously obtained results in the paper in Ref. [18]. Measurements of the temperature dependences of the magnetization of Fe_7S_8 compound revealed a magnetic phase transition from a ferrimagnetic state to a paramagnetic one at 590 K, which was established earlier in Ref. [1].

NMR measurements on ^{57}Fe nuclei (natural abundance of the isotope) were performed using pulsed spectrometer in a zero external magnetic field in the temperature range from 4.2 to 300 K. NMR spectra on ^{57}Fe nuclei were obtained using the standard spin echo technique $p{-}t_{del}{-}p{-}t_{del}{-}echo$. The copper coil with the sample had a diameter of 5 mm. The pulse duration $p = 1\,\mu$s was selected, the RF amplifier power was $W \approx 10{-}20$ W.

The NMR spectra on ^{57}Fe nuclei presented in this paper constitute the integral intensity of the received *echo*-signals accumulated in the required frequency range in steps of $\Delta\nu = 200{-}250$ kHz. The spectra were recorded with a delay between pulses of $t_{del} = 40\,\mu$s. The number of accumulations at $T = 77$ K was 6080 at each point and it was 25000 at $T = 295$ K. The pulse sequence was repeated after $4 \times T_1$, where T_1 is the spin-lattice relaxation time. The achieved signal-to-noise ratio at the frequency corresponding to the maximum of the NMR spectrum was at least 30. The original program „Simul“ [19] was used to model the NMR spectra, which makes it possible to numerically calculate the shape of the line based on the complete Hamiltonian of the nuclear system, taking into account the Zeeman contribution [20,21].

The spin-spin relaxation time T_2 was measured at peak maxima with a change of the delay time between pulses t_{del} in the pulse sequence of the spin echo. The spin-spin relaxation times were well approximated by the expression:

$$M(2t_{del}) = M_0 \times \exp(-2t_{del}/T_2). \quad (1)$$

The spin-lattice relaxation times T_1 on ^{57}Fe nuclei were also measured at line maxima by inversion-recovery method. The pulse sequence $2p{-}t_{inv}{-}p{-}t_{del}{-}p{-}t_{del}{-}echo$ was used with a constant delay of $t_{del} = 40\,\mu$s for measuring T_1. The number of points on the nuclear magnetization recovery curve was at least 35. The recovery of nuclear magnetization was well described by an exponential function in the entire temperature range studied:

$$[M_0 - M_z(t_{inv})]/[M_0 - M_z(t_{inv} = 0)] = \exp(-t_{inv}/T_1), \quad (2)$$

where M_0 is the equilibrium value of the longitudinal nuclear magnetization $M_z(t)$, i. e. at $M_0 = M_z(t_{inv} = \infty)$.

3. Results and discussion

The complexity of observing NMR on nuclei of iron ^{57}Fe with spin $I = 1/2$ in the magnetically ordered state of matter is attributable to the low natural abundance of ^{57}Fe NMR isotope, which is only 2.1%, and very short spin-spin relaxation times. Since the magnetic iron ions inside the cationic layers are ferromagnetically ordered in pyrrhotite Fe_7S_8, the registration of the NMR signal from the ^{57}Fe nuclei inside the domains and their walls becomes possible due to the mechanisms of its significant amplification [22,23].

Figure 2 shows NMR spectra on ^{57}Fe nuclei in a polycrystalline sample of Fe_7S_8 in a zero external magnetic field at three temperatures: 4.2, 77, 295 K. NMR spectra on ^{57}Fe nuclei are in the frequency range characteristic of iron ions in Fe^{2+} state [15,23]. The frequency range of $\Delta\nu = 20{-}80$ MHz was scanned during the experiments and no other signals were detected besides those shown in Figure 2, which indicates the absence of iron ions in Fe^{3+} state. This conclusion is consistent with the data of Mossbauer spectroscopy [9–11], X-ray magnetic circular

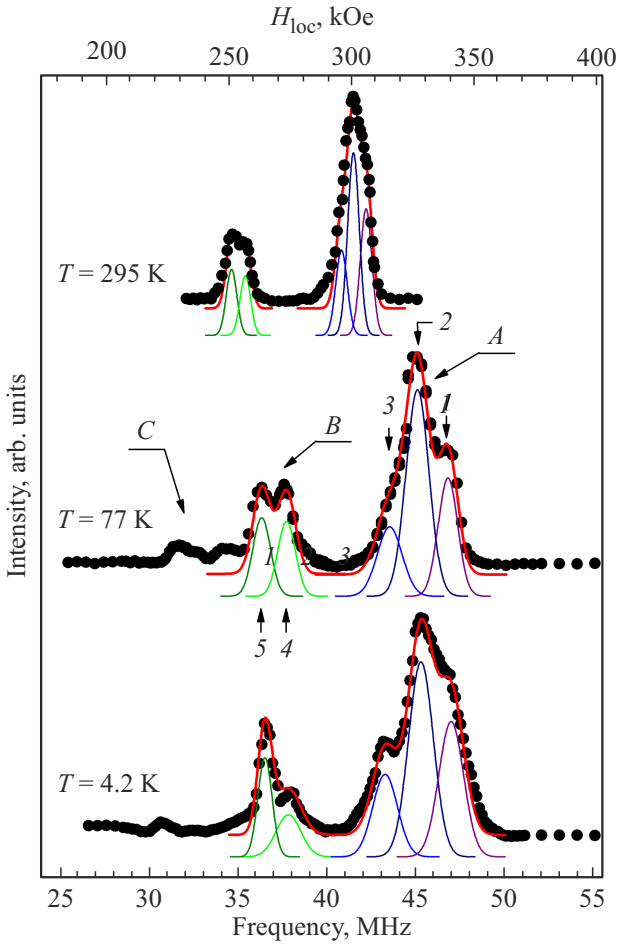

Figure 2. NMR spectra on ^{57}Fe nucleus at three temperatures of 4.2, 77, 295 K in a zero external magnetic field. The result of data modeling with three lines are shown by the solid red line.

The times of spin-spin T_2 and spin-lattice T_1 relaxations and the values of local magnetic fields at the location of ^{57}Fe nuclei corresponding to different frequency ranges of the NMR spectrum and temperatures

T, K	T_1, ms		T_2, ms		$H_{loc}(\Delta\nu_1)$, kOe			$H_{loc}(\Delta\nu_2)$, kOe		$H_{loc}(\Delta\nu_3)$, kOe
	$\Delta\nu_1$	$\Delta\nu_2$	$\Delta\nu_1$	$\Delta\nu_2$	1	2	3	4	5	
4.2	5.6	5.3	0.165	0.155	341.2	328.9	314.3	274.7	265.1	223.8
77	16.1	14.9	8.38	8.36	339.8	327.3	316.0	273.7	263.6	230.8
295	4.4	4.2	0.520	0.460	306.3	301.1	296.2	257.1	251.2	–

dichroism [24,25] and the results of studies using powder neutron diffraction [2].

Three subspectrums can be distinguished in the NMR spectrum of ^{57}Fe nuclei (let's call them A, B and C) in the frequency ranges of $\Delta\nu_1 = 40-50$ MHz, $\Delta\nu_2 = 35-38$ MHz and $\Delta\nu_3 = 31-34$ MHz. The NMR spectra in the $\Delta\nu_1$ and $\Delta\nu_2$ ranges can only be modeled using three and two lines, respectively. Local magnetic fields $H_{loc,i} = \nu_i/^{57}\gamma$ at the location of ^{57}Fe nuclei corresponding to different frequency ranges of the NMR spectrum were calculated using the gyromagnetic ratio of iron $^{57}\gamma/2\pi = 1.378$ MHz/T. Here ν_i are the resonant frequencies of the NMR lines (see Figure 2). The values of these fields are listed in the table.

Figure 3 shows the dependences of the amplitude of the spin echo $M(2t_{del})$ on the doubled delay between pulses t_{del} and dependence of the value $(M_0 - M_z(t_{inv}))/(M_0 - M_z(t_{inv} = 0))$ on t_{inv} in two sections of the NMR spectrum of ^{57}Fe nuclei at temperatures of 295 and 77 K. The figure shows that both the amplitude drop $M(2t_{del})$ and the values $(M_0 - M_z(t_{inv}))/(M_0 - M_z(t_{inv} = 0))$ measured in the frequency ranges of $\Delta\nu_1$ and $\Delta\nu_2$ at the same temperature are quite close to each other. As is known, the rate of spin-lattice relaxation $1/T_1$ is proportional to the square of the transverse component $H_{loc}^{\perp}$ of the local magnetic field on the nucleus [20,21]. Then the approximate equality of $H_{loc}^{\perp}$ for the nuclei at positions A and B, but the difference of their values H_{loc}^{z} may indicate a slight anisotropy of these fields on iron nuclei at least one of the site.

The times of spin-spin T_2 and spin-lattice T_1 relaxation were determined as a result of processing of dependencies $M(2t_{del})$ and $(M_0 - M_z(t_{inv}))/(M_0 - M_z(t_{inv} = 0))$ by functions (1) and (2). The data obtained are listed in the table. It can be said based on the three temperature points that the relaxation dependences are nonmonotonic in nature and require further systematic measurements at intermediate temperatures.

The value of the local field $H_{loc} = 301.1(4)$ kOe, corresponding to the line 2 at room temperature was taken to estimate the magnetic moment of iron ions corresponding to the high-frequency NMR line ($\Delta\nu_1$). We obtain $\mu \approx 2.38\,\mu_B$ using a simple relationship between the local magnetic field on H_{loc} nucleus and the ion magnetic moment μ, $H_{loc} = A\mu$,

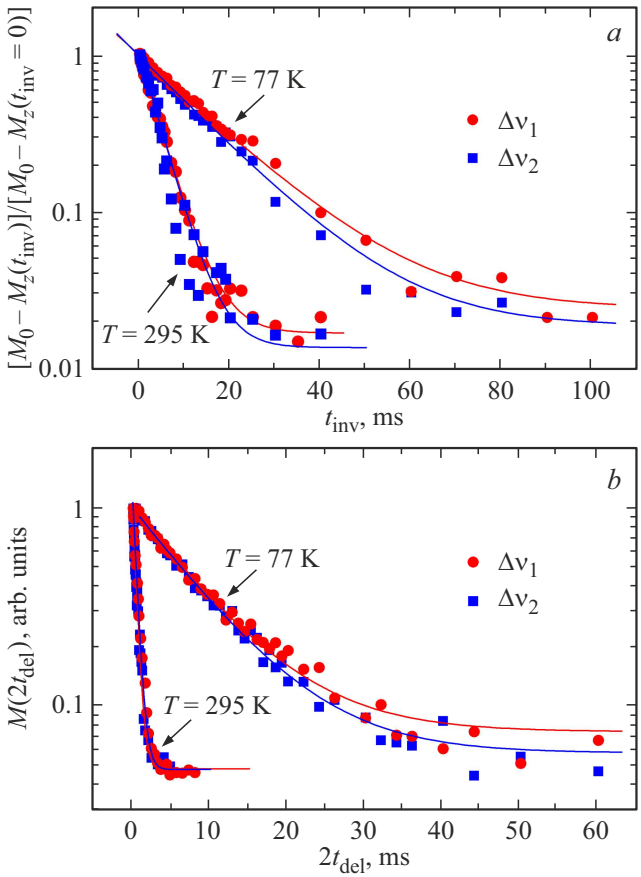

Figure 3. Data from measurements of relaxation times T_1 and T_2 in different parts of ^{57}Fe NMR spectrum ($\Delta\nu_1$ and $\Delta\nu_2$) at temperatures of $T = 295$ K and $T = 77$ K in Fe_7S_8. *a*) The value $(M_0 - M_z(t_{inv}))/(M_0 - M_z(t_{inv} = 0))$ depending on the delay between pulses t_{inv}. The data approximation by expression (2) is shown by solid curves. *b*) Dependence of the amplitude of the spin echo $M(2t_{del})$ on the doubled delay between pulses t_{del} in the pulse sequence of the spin echo. The data approximation by expression (1) is shown by solid curves.

where $A = -125$ kOe/μ_B is a known hyperfine interaction constant of 3*d*-electrons [26]. This value is in good agreement with the results of papers in Refs. [1,2,27–30], where $\mu \approx 2.03-2.5\,\mu_B$. The low value of the magnetic moment μ and the absence of iron ions in the compound in the Fe^{3+} state indicate that pyrrhotite Fe_7S_8 is not described

by a simple ion model assuming the existence of well-localized 3*d*-electrons and, accordingly, localized magnetic moments [1]. There is a critical value of the cation-cation distance according to Ref. [31], below which the 3*d*-orbitals of iron atoms overlap and partial delocalization of 3*d*-electrons occurs. This critical value is 3 Å for $Fe_{1-x}S$ system and such small lengths of Fe-Fe bond are present in pyrrhotite Fe_7S_8 (see [1] for example). The existence of such bonds may increase the stability of $Fe_7^{2.29+}S_8^{2-}$ ion model [32].

The presence of three different frequency ranges of $\Delta\nu_1$, $\Delta\nu_2$ and $\Delta\nu_3$, in which the NMR signal from ^{57}Fe is observed, indicates the presence of at least three substantially magnetically unequal Fe ions in Fe_7S_8. The decomposition with several values of hyperfine fields was also used in studies using the Mossbauer spectroscopy [9–11]. The authors attribute these fields to the crystallographic inequivalence of iron ions and the number of vacancies near them. Theoretical and experimental studies of FeS compound [31,33] show that the magnetic bond between iron ions lying in the same magnetic plane is much weaker than the interplanar bonds. Moreover, the interplane cation-anion-cationic superexchange interaction prevails over the cation-cationic interactions on ions with a more than half-filled *d*-shell [31]. A rough model of magnetic interactions was proposed in Ref. [11], in which all intraplane cation-cation interactions were neglected, and all predominant interplane superexchange bonds Fe-S-Fe were considered the same.

Let us consider qualitatively the ordering of vacancies in the 4*C*-type superstructure shown in Figure 1. Such a structure implies a sequential alternation of layers of iron without vacancies and with vacancies ordered in a certain way. Each iron ion has two vacancies in „its“ plane in its immediate environment in layers where there are ordered vacancies and none in its two neighboring layers (the neighboring upper and lower layers have no vacancies, see Figure 1). Moreover, there are two crystallographically inequivalent iron sites A_1 and A_2 in the layers with vacancies (Figure 1, *b*). Their inconsistency is attributable to the varying degrees of distortion of the sulfur atom octahedra surrounding the iron ions at sites A_1 and A_2, as well as the length of the Fe-Fe bonds. The presence of such distorted octahedra FeS_6 has been noted in a number of studies of Fe_7S_8 using various methods [2,9–11,32]. Each Fe ion occupying the position A_1 or A_2 interacts with seven Fe ions in the neighboring layer through nine superexchange bonds: three with the nearest Fe ion and six with iron ions arranged hexagonally around this nearest ion. At the same time, vacancies do not affect iron in positions A_1 and A_2, since all intraplane interactions are so small that they can be ignored [32]. This is also confirmed by the Mossbauer studies [7,9–11,34], which showed that the local magnetic fields are equal ($H_{loc} \approx 300$ kOe) on the Fe nuclei at positions A_1 and A_2 in Fe_7S_8 and in the FeS troilite, where there are no vacancies. The nonequivalence of the lines corresponding to positions A_1 or A_2 in the Mossbauer spectra is most clearly manifested at low temperatures because of the different temperature behavior of hyperfine fields at each sites. The same value $H_{loc} \approx 300$ kOe was obtained for iron resonating in the frequency range of $\Delta\nu_1$. This makes it possible to assign the NMR spectrum at these frequencies to the iron sites A_1 and A_2. The division of the NMR spectrum in the frequency range $\Delta\nu_1$ into three lines can be attributed primarily to the positions A_1 and A_2, the origin of the third line remains unclear. Nevertheless, the existence of additional lines in the spectra may be caused by the structurally inhomogeneous state of the polycrystalline sample of $Fe_{7\pm\delta}S_8$. It should be noted that only one asymmetric line was observed in Fe_7S_8 in the first NMR study of ^{57}Fe nuclei [13]. The reason for this asymmetry has not been analyzed by the authors in any way.

Let us now consider the iron ions located in the planes where there are no vacancies: sites *B* and *C* [11]. The iron positions *B* have two vacancies in the immediate environment in neighboring layers, „diagonally“ located along the directions [1, 1, 0] in the upper layer and along the directions [1, −1, 0] in the lower layer. The iron positions *C* have two diagonal vacancies in one adjacent layer like positions *B* but only one vacancy is located directly above (below) the sites *C* in the other adjacent layer. Iron ions at sites *B* are bound to Fe ions in two adjacent planes by fourteen of the eighteen possible Fe-S-Fe bonds due to the presence of vacancies, and ions at sites *C* are bound to Fe ions by thirteen such bonds. Therefore, we should expect lower values of hyperfine fields for these ions in comparison with the values for the subspectrum *A*. Consequently, the resonant frequencies are also lower. Therefore, the subspectrums *B* and *C* in the frequency range $\Delta\nu_2$ and $\Delta\nu_3$ can be associated with iron nuclei at positions *B* and *C*, respectively. It is noteworthy that there is some discrepancy between the relative intensities of the lines *A*, *B* and *C*. The total number of nuclei in positions *B* and *C* is 1.14 times greater than in positions *A*, and the total intensity of the lines *B* and *C* is less than the intensity lines *A*. Moreover, the intensities of the lines *B* and *C* should be comparable in magnitude, since the quantity of sites *B* and *C* is the same. However, this is not observed experimentally. The possible reason is that the intensity of the NMR spectrum strongly depends on a variety of experimental details of spectral measurements. For example, the sensitivity of our equipment decreases significantly in the low frequency range, where NMR from iron nuclei is observed at sites *B* and especially *C*. Moreover, both the *Q*-factor of the oscillatory circuit *Q* and the gain factor η depend on the frequency, which have a strong effect on the intensity of the NMR signal. As a result, quite significant discrepancies may be possible between the expected and actual intensities of NMR lines when measuring spectra in a wide frequency range.

Thus, the ^{57}Fe spectra in Fe_7S_8 chalcogenide can be interpreted, at least qualitatively, in the model of 4*C*-type superstructure. At least, it is safe to say that vacancies in Fe_7S_8 are distributed not statistically evenly, but in an

orderly manner. Our results on local magnetic fields (see table) are in good agreement with the data from studies performed using Mossbauer spectroscopy [7,11,34]. A more accurate identification of the lines corresponding to different immediate environments of iron ions requires additional other compositions and systematic NMR studies on ^{57}Fe nuclei as was done, for example, in Ref. [35].

This study also makes it possible to further optimize the technology for detecting materials containing Fe_7Se_8, since the NMR method on ^{57}Fe nuclei can be appropriately adapted to detect and select ore fragments containing pyrrhotite. For instance, recording of NMR signals using Carr-Purcell or Carr-Purcell-Meiboom-Gill pulse sequences can be considered to increase the signal [36–38]. The use of these sequences will significantly reduce the signal accumulation time at the peak resonant frequency of 42 MHz.

4. Conclusion

An NMR study of layered chalcogenide Fe_7S_8 (pyrrhotite) in a magnetically ordered state in a zero external magnetic field was performed using ^{57}Fe nuclei as NMR probes. The NMR spectrum on the ^{57}Fe nucleus is a line of complex shape with several maxima in the frequency range of $\Delta\nu = 30-50$ MHz. The spin-spin and spin-lattice relaxation rates of nuclear magnetic moments of ^{57}Fe have been determined at different frequency regions of the spectrum at different temperatures. Analysis of NMR spectra on ^{57}Fe nuclei showed the presence of several magnetically nonequivalent iron ion sites with different number and location of vacancies near them. Local magnetic fields on iron nuclei were measured and the magnetic moment on Fe ions was estimated. Evidence of the formation of a vacancy superstructure of the 4*C*-type in Fe_7S_8 has been found.

The relaxation parameters of the nuclear magnetic moments of iron obtained in this study make it possible to expand the use of NMR spectroscopy in the mining industry, for example, for the detection, separation and real-time selection of ore fragments containing pyrrhotite (Fe_7S_8). In particular, NMR can be used for the extraction of iron-nickel pyrite, the ore of which also contains pyrrhotite. The use of Carr-Purcell sequences or an improved version of Carr-Purcell-Meiboom-Gill [36–38] will significantly reduce the accumulation time of the NMR signal.

Acknowledgments

The work was performed using the equipment of CUC „Testing Center for Nanotechnology and Advanced Materials“ and „Department of Cryogenic Technologies“ of Institute of Metal Physics of Ural branch of RAS.

Funding

The study was carried out at the expense of a grant from the Russian Science Foundation (project No. 22-12-00220).

Conflict of interest

The authors declare the absence of conflicts of interest.

References

[1] H. Wang, I. Salveson. Phase Transitions **78**, 547 (2005).
[2] A.V. Powell, P. Vaqueiro, K.S. Knight, L.C. Chapon, R.D. Sánchez. Phys. Rev. B **70**, 014415 (2004).
[3] W. O'Reilly, V. Hoffmann, A.C. Chouker, H. C. Soffel, A. Menyeh. Geophys. J. Int. **142**, 669 (2000).
[4] F. Li, H.F. Franzen, M.J. Kramer. J. Solid State Chem. **124**, 264 (1996).
[5] N.V. Baranov, P.N.G. Ibrahim, N.V. Selezneva, V.A. Kazantsev, A.S. Volegov. D.A. Shishkin. Physica B: Condens. Matter **449**, 229 (2014).
[6] N.V. Baranov, P.N.G. Ibrahim, N.V. Selezneva, A.F. Gubkin, A.S. Volegov, D.A. Shishkin, L. Keller, D. Sheptyakov, E.A. Sherstobitova. J. Phys. Condens. Matter **27**, 286003 (2015).
[7] T. Ericsson, Ö. Amcoff, P. Nordblad. Hyperfine Interact. **90**, 515 (1994).
[8] P. Terzieff. J. Phys. Chem. Solids **43**, 305 (1982).
[9] J.R. Gosselin, M.G. Townsend, R.J. Tremblay, A.H. Webster. Mater. Res. Bull. **10**, 41 (1975).
[10] D.J. Vaughan, M.S. Ridout. Solid State Commun. **8**, 2165 (1970).
[11] L.M. Levinson, D. Treves. J. Phys. Chem. Solids **29**, 2227 (1968).
[12] T.J. Bastow, A. Trinchi. Solid State Nucl. Magn. Reson. **35**, 25 (2008).
[13] T.J. Bastow, A.J. Hill. J. Magn. Magn. Mater. **447**, 58 (2018).
[14] J.A. Lehmann-Horn, D.G. Miljak, L.A. O'Dell, R. Yong, T.J. Bastow. Geophys. Res. Lett. **41**, 6765 (2014).
[15] T.J. Bastow, A. Trinchi, M.R. Hill, R. Harris, T.H. Muster. J. Magn. Magn. Mater. **321**, 2677 (2009).
[16] D.F. Akramov, N.V. Selezneva, P.N.G. Ibrahim, V.V. Maikov, E.M. Sherokalova, D.K. Kuznetsov, N.V. Baranov. Phys. Met. Metallogr. **123**, 282 (2022).
[17] N. Selezneva, P. Ibrahim, N.M. Toporova, E.M. Sherokalova, N. Baranov. Acta Phys. Pol. A **133**, 450 (2018).
[18] D. Koulialias, B. Lesniak, M. Schwotzer, P.G. Weidler, J.F. Löffler, A.U. Gehring. Geochem. Geophys. Geosystems **20**, 5216 (2019).
[19] A.P. Gerashchenko, S.V. Verkhovsky, A.F. Sadykov, A.G. Smolnikov, Yu.V. Piskunov, K.N. Mikhalev. Certificate of state registration of a computer program № 2018663091. Simul 2018, Registered in the Register of Computer Programs on 22.10.2018.
[20] C.P. Slichter. Principles of Magnetic Resonance. Springer Science & Business Media, (1996). 658 p.
[21] A. Abragam. The Principles of Nuclear Magnetism. Clarendon Press, (1961). 599 p.
[22] A.M. Portis, A.C. Gossard. J. Appl. Phys. **31**, S205 (1960).

[23] V.V. Ogloblichev, V.I. Izyurov, Y.V. Piskunov, A.G. Smol'nikov, A.F. Sadykov, S.A. Chuprakov, S.S. Dubinin, S.V. Naumov, A.P. Nosov. JETP Letters **114**, 29 (2021).
[24] I. Letard, P. Sainctavit, C. Deudon. Phys. Chem. Miner. **34**, 113 (2007).
[25] V.N. Antonov, L.V. Bekenov, A.P. Shpak, L.P. Germash, A.N. Yaresko, O. Jepsen. J. Appl. Phys. **106**, 123907 (2009).
[26] A.J. Freeman, R.R. Frankel. Hyperfine Interactions. Academic Press, New York and London (1967). 758 p.
[27] C. Haines, S. Dutton, M. Volk, M. Carpenter. J. Phys. Condens. Matter **32**, 405401 (2020).
[28] E.J. Schwarz. J. Geomag. Geoelec. **20**, 67 (1968).
[29] R. Benoit. J. Chim. Phys. **52**, 119–132 (1955).
[30] M. Bin, R. Pauthenet. J. Appl. Phys. **34**, 1161 (1963).
[31] J.B. Goodenough. J. Appl. Phys. **33**, 1197 (1962).
[32] M. Tokonami, K. Nishiguchi, N. Morimoto. Am. Mineral. **57**, 1066 (1972).
[33] E. Hirahara, M. Murakami. J. Phys. Chem. Solids **7**, 281 (1958).
[34] C. Jeandey, J.L. Oddou, J.L. Mattei, G. Fillion. Solid State Commun. **78**, 195 (1991).
[35] O. Kruse. Am. Mineral. **75**, 755 (1990).
[36] Impul'snaya i fur'e-spektroskopiya YaMR. Per. s angl. B.A. Kvasov; pod red. E.I. Fedin. Mir, M. (1973). 164 p. (in Russian).
[37] H.Y. Carr, E.M. Purcell. Phys. Rev. **94**, 630 (1954).
[38] S. Meiboom, D. Gill. Rev. Sci. Instrum. **29**, 688 (1958).

Translated by A.Akhtyamov